INSTITUT DE FRANCE
Académie des sciences

Comptes Rendus
Chimie

Raphaël Lamare, Romain Ruppert, Mourad Elhabiri, Gilles Ulrich, Laurent Ruhlmann and Jean Weiss

Design and synthesis of charged porphyrin dimers for polyoxometalate recognition

Volume 24, Special Issue S3 (2021), p. 115-126

Published online: 17 August 2021
Issue date: 16 December 2021

https://doi.org/10.5802/crchim.105

Part of Special Issue: MAPYRO: the French Fellowship of the Pyrrolic Macrocyclic Ring

Guest editors: Bernard Boitrel (Institut des Sciences Chimiques de Rennes, CNRS-Université de Rennes 1, France) and Jean Weiss (Institut de Chimie de Strasbourg, CNRS-Université de Strasbourg, France)

This article is licensed under the
Creative Commons Attribution 4.0 International License.
http://creativecommons.org/licenses/by/4.0/

Les Comptes Rendus. Chimie *sont membres du*
Centre Mersenne pour l'édition scientifique ouverte
www.centre-mersenne.org
e-ISSN : 1878-1543

Comptes Rendus
Chimie
2021, 24, nº S3, p. 115-126
https://doi.org/10.5802/crchim.105

MAPYRO: the French Fellowship of the Pyrrolic Macrocyclic Ring / *MAPYRO: la communauté française des macrocycles pyrroliques*

Design and synthesis of charged porphyrin dimers for polyoxometalate recognition

Raphaël Lamare [a], **Romain Ruppert** [a], **Mourad Elhabiri** [b], **Gilles Ulrich** [c], **Laurent Ruhlmann** *, [a] and **Jean Weiss** *, [a]

[a] Institut de Chimie de Strasbourg, UMR 7177 CNRS-Université de Strasbourg, 4 rue Blaise Pascal, 67000 Strasbourg, France

[b] Equipe Chimie Bioorganique et Médicinale, Laboratoire d'Innovation Moléculaire et Applications (LIMA), UMR7042, CNRS-Unistra-UHA, European School of Chemistry, Polymers and Materials (ECPM), 25, rue Becquerel, 67087 Strasbourg, France

[c] ICPEES - Institut de Chimie et Procédés pour l'Énergie, l'Environnement et la Santé, ECPM, 25 rue Becquerel, 67087 Strasbourg, France

E-mails: raphael.lamare@etu.unistra.fr (R. Lamare), rruppert@unistra.fr (R. Ruppert), elhabiri@unistra.fr (M. Elhabiri), gulrich@unistra.fr (G. Ulrich), lruhlmann@unistra.fr (L. Ruhlmann), jweiss@unistra.fr (J. Weiss)

Abstract. A series of porphyrin dimers have been prepared and characterized in order to form inclusion complexes with Lindqvist-type polyoxometallates. The synthesis of the porphyrin dimer has been optimized and can serve general purposes. The formation of inclusion complexes has been monitored using spectroscopic methods and moderate affinities with log K_{assoc} varying from 2.6 to 4.2 have been determined and the parameters governing the formation of the complexes have been examined.

Keywords. Porphyrins, Polyoxometalates, Molecular recognition, Fluorescence quenching, Host–guest chemistry.

Available online 17th August 2021

1. Introduction

Polyoxometalates (POMs) have been widely studied in photovoltaic applications and in the design of electroactive materials despite their absorption in the 200–400 nm region that is a significant drawback regarding their efficiency. This inconvenience has been mostly circumvented by the use of sensitizers, that absorbs in the visible region, able to transfer electrons to POMs. Among these sensitizers, porphyrins that offer the advantages of strong absorption coefficients in the visible domain have been used in efficient, but rather undefined, assemblies generated by polymerization at the surface of electrodes [1,2]. Discrete species can be prepared by several covalent methods. In polyoxomolybdates [3–6] and polyoxovanadates [7], replacing one or several peripheral hydroxyl groups by alkoxy groups of a linker already connected to a porphyrin unit has proven to

* Corresponding authors.

be efficient on several occasions, leading to scaffolds with photocatalytic activity. In the case of polyoxotungstates, it is also possible to substitute an oxo-group by a transition metal ion that will coordinate a peripheral ligand introduced on a porphyrin [8]. Coordination chemistry has been employed taking advantage of the Lewis acidity of metal ions incorporated in the porphyrin core [9,10], however, due to the highly negative charge of the POMs, electrostatic interactions have emerged as an efficient self-assembly driving force in the field of porphyrin/POM hybrids [11–13]. Despite their performances in photo-induced processes, materials built on electrostatic interactions are structurally poorly defined [14–16] which limits the scope of optimization based on molecular properties. Well-defined species provide information on interactions at the molecular scale and a reliable insight on the performance of the resulting molecular materials.

2. Results and discussion

Supramolecular chemistry and its toolbox of non-covalent interactions combined with host–guest principles of molecular recognition provide tools for the design of hosts adapted for the binding of diversely shaped polyoxomolybdates. In an attempt to provide a rational approach to the formation of well-defined porphyrin/POM hybrids, charged bis-porphyrinic receptors have been synthesized and used in binding studies of Lindqvist-type POMs. The design of pre-organized porphyrin dimers able to develop controlled interactions with polyoxometalates is described hereafter. In order to introduce charges on the porphyrin dimers, two options were possible and are summarized in Figure 1. Introduction of charges at the position marked in green ($X = N^+$) *via* nucleophilic addition of a pyridine group on a porphyrin radical cation, obtained by chemical or electrochemical oxidation of a triarylporphyrin, failed for mechanistic reasons [17], and thus the introduction of charges in the positions marked in red ($Y = N^+$) has been developed (Figure 1).

Two main synthetic methods have been developed. The first dealt with the stepwise functionalization of the linker and the formation of the series of compounds represented in Scheme 1.

The yields of porphyrins **3**, **4**, **5** and **6** have been optimized through the testing of a variety of solvents at room temperature and reflux. It must be noted that some loss of compound occurs during the anion exchange that follows the quaternization of the pyridine group. The porphyrins **3**, **4**, **5** and **6** can be involved as alkylating agent for a second quaternization of either **1** or **2** in refluxing THF over 30 h to lead to the bis-porphyrins **7**, **8**, **9**, **10** represented in Figure 2.

The same series of compounds can be obtained by the second approach that consists in reacting an excess of the porphyrins **1** or **2** with the appropriate α,α'-dibromoxylene in refluxing THF. This direct method afforded the doubly charged bis-porphyrins **7**, **8**, **9** and **10** in 46%, 38%, 46% and 32% yield, respectively. Although all the bis-porphyrins were intended to form tweezers in which the two porphyrins are facing each other, all characterization methods suggested that the compounds adopt an extended conformation in solution, as shown, for example, by the ^{1}H NMR spectrum of **7** in DMSO (Figure 3). In this spectrum, no anisotropic shielding of the porphyrin protons due to stacking is observed and all signals appear at chemical shifts typical of independent porphyrins.

Primary modelling has been performed using Spartan (MM2) for **9Zn$_2$** and three different template guests, namely 4,4′-bipyridine, 4,4′-dipyridylacetylene, and 4-(*p*-phenyl-4-pyridyl)-pyridine, to evaluate the most favourable size for a guest in the hypothetical zinc(II) complexes. The structure calculated for 4,4′-dipyridylacetylene as a guest is depicted in Figure 4. The series of calculated structures suggested that in a cofacial conformation of the two porphyrins, an energy minimum should be reached for a distance somewhere between 11 and 14 Å for **9Zn$_2$** although all structures have proven to be quite flexible. For this reason, the choice of POM guest for this study rested on a Lindqvist-type entity in which the distance between terminal oxygen atoms is 8 Å (X-ray diffraction) [18]. The inclusion of Lindqvist POM ($[Mo_6O_{19}]^{2-}$) in bis-porphyrins has been investigated by various methods. UV–visible absorption titrations were judged not suitable due to the absence of noticeable spectral variations upon addition of guest. However, fluorescence quenching experiment and excited state lifetime measurements on the porphyrin dimers and electrochemistry provided insightful information on the recognition process.

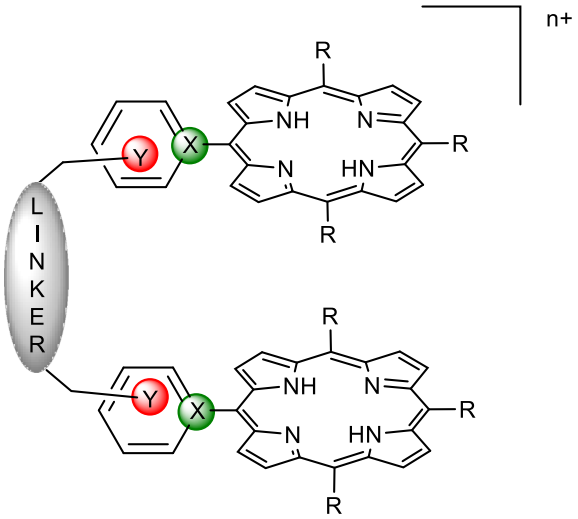

Figure 1. Targeted charged bis-porphyrins and two possible charge localizations (X or Y = tetravalent N).

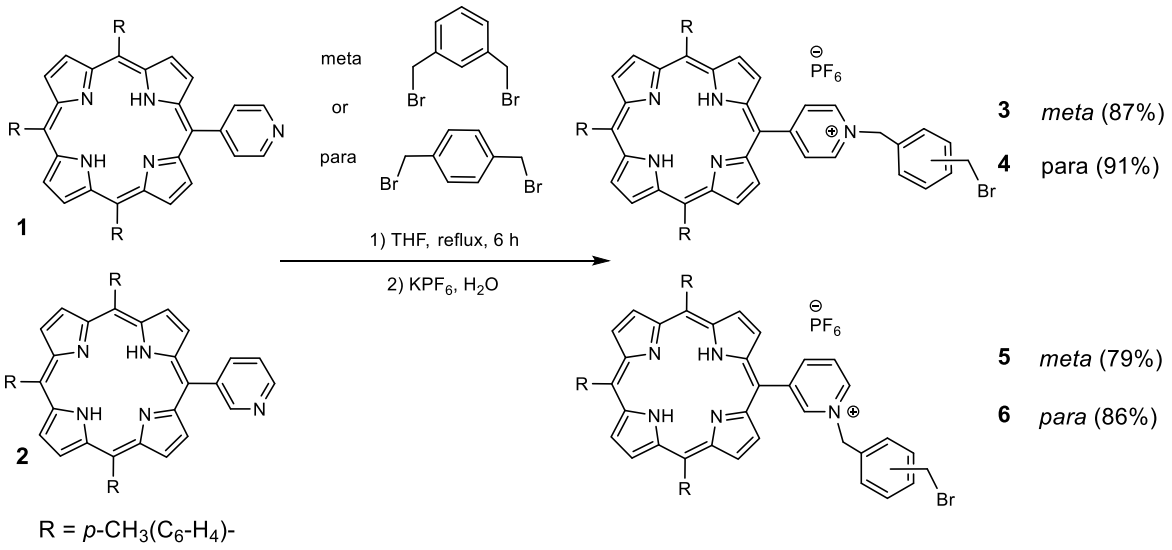

Scheme 1. Synthesis of bis-porphyrin precursors **3**–**6**.

3. Fluorescence quenching titrations

Fluorescence quenching experiments have been performed on hosts **3**–**6** and **7**–**10** to determine the highest association constant. For the strongest porphyrin/POM association, excited state lifetime measurements have been performed. Figure 5(a) represents a typical evolution of the porphyrin emission observed during the titration of **9** (6.43×10^{-6} M) with $[Mo_6O_{19}][(n\text{-Bu})_4N]_2$ (1.76×10^{-2} M). Monitoring the decrease of the intensity for both emission bands centred at 652 and 712 nm upon addition of the POM guest lead to the plot in Figure 5(b) which confirms that the emission decrease at 652 nm is not the sole result of dilution. The same trend is observed for the band at 712 nm. The analysis of these data using the Specfit program yielded an association constant K with a log value of 4.20 ± 0.03

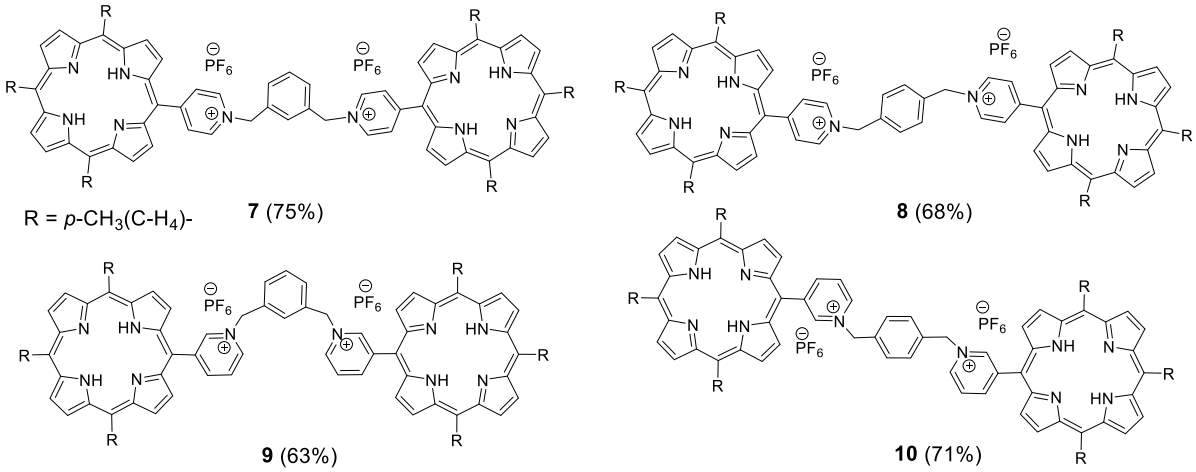

Figure 2. Series of doubly charged porphyrin dimers obtained by stepwise quaternization.

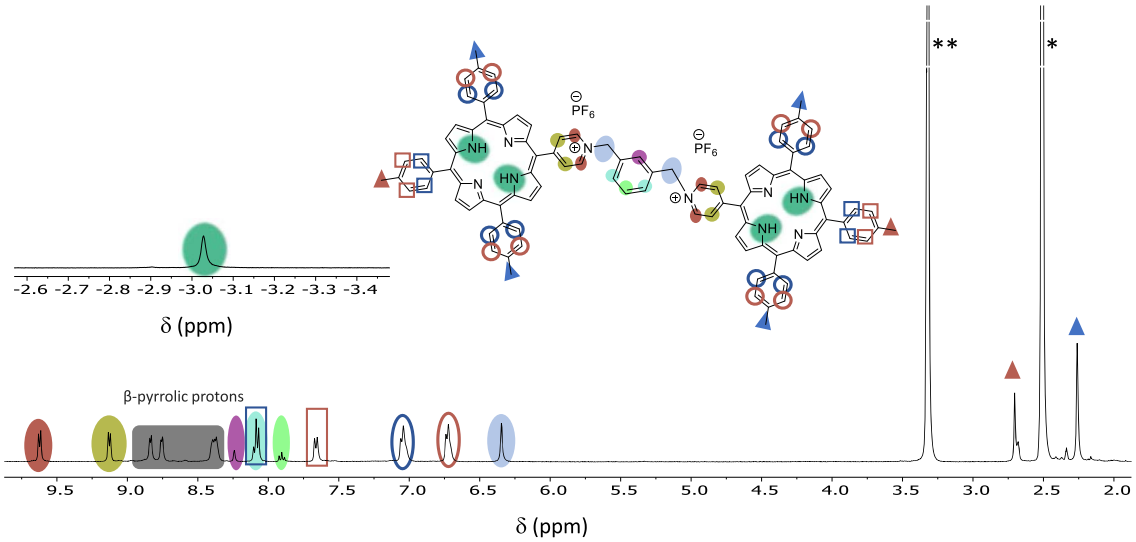

Figure 3. ^{1}H NMR of **7** at 300 MHz in DMSO-d_6 (298 K). (*) Residual non deuterated solvent and (**) H_2O.

for a complex **9**-POM with a 1:1 stoichiometry. The corresponding Job plot is available in the supporting information (Figure S51), and the distribution curve (Figure S46 in the ESI) shows that a maximum of 95% of host–guest complex is formed in the presence of large excess of POM (ca. 340 eq).

The behaviour of **9** has been compared with the behaviour of a single porphyrin derivative such as **6**, and, interestingly, the fluorescence quenching seems globally more efficient in the case of the single porphyrin **6** (Figure 6). The residual emission observed at the end of the titration is indeed probably due to free porphyrin **6** because of the experimental conditions for which only about 65% of 6-POM complex is formed (Figure S47 in the ESI). In addition, the monitoring of the decrease clearly suggests that the association process is less efficient than in the case of the dimer (log $K = 2.4 \pm 0.1$ for **6**-POM versus log $K = 4.20 \pm 0.03$ for **9**-POM as determined by Specfit). Thus, a reasonable hypothesis is that the single porphyrin **6** has more degrees of freedom and is able to establish some close contact with the POM for efficient excited

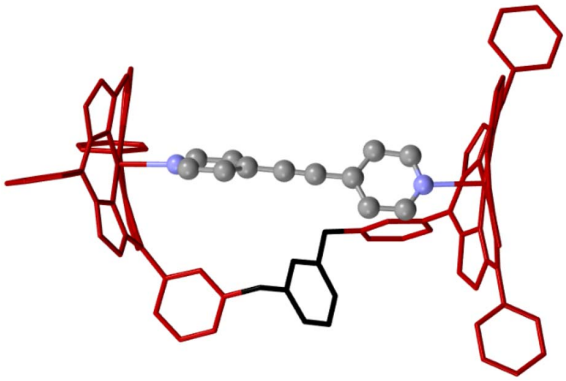

Figure 4. Artificially folded calculated structure of a coordination complex of **9Zn$_2$** with 4,4′-dipyridylacetylene. Colour code: Burgundy = porphyrin, black = spacer, ball and stick = guest.

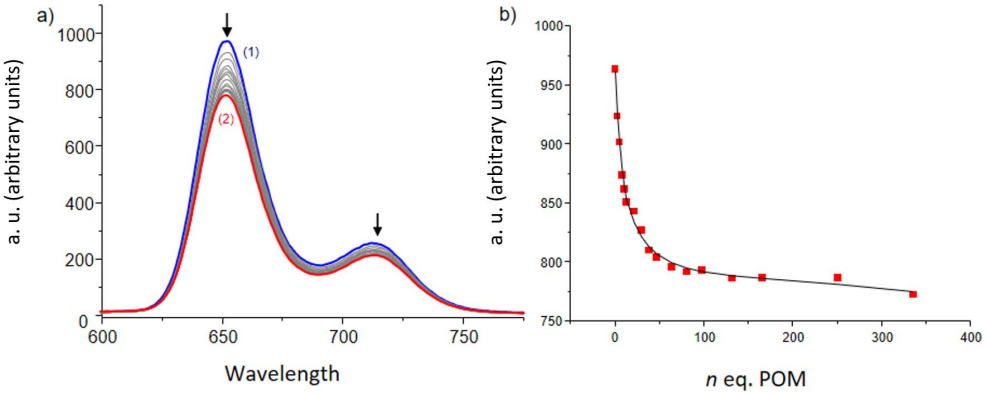

Figure 5. (a) Fluorescence titration of **9** with $[Mo_6O_{19}][(n\text{-Bu})_4N]_2$. Solvent: DMF, T = 25.0 °C, λ_{ex} = 517 nm, emission and excitation slits 15/20 nm, (1) [**9**] = 6.43 × 10^{-6} M; (2) [POM]/[**9**] = 340. (b) Monitoring of the emission intensity at 652 nm as a function of the number of $[Mo_6O_{19}][(n\text{-Bu})_4N]_2$ equivalents. The absorption spectra are not corrected from dilution effects.

Table 1. Solvent DMF, T = 25.0 °C, λ_{ex} = 517 (±1) nm, (error) equal to 1 σ (standard deviation)

Compound	Porphyrin **3**	Bis-por **7**	Porphyrin **4**	Bis-por **8**	Porphyrin **5**	Bis-por **9**	Porphyrin **6**	Bis-por **10**
log $K(\sigma)$	2.8(1)	2.7(1)	2.7(1)	3.3(1)	2.8(1)	4.20(3)	2.4(1)	2.6(2)

state quenching whereas, in the dimer, the presence of the spacer introduces some restraints preventing both porphyrins from getting in close contact with the POM guest or forcing only one of the porphyrin to be quenched by the POM guest thus explaining the significant residual of emission **9**-POM (Figure S46 in the ESI). It should be noted that for all single porphyrin derivatives, stoichiometry has been difficult to assign due to the level of error in the data and the weakness of most association constants and the latter have been determined for a 1/1 stoichiometry for comparison. A summary of the association constants is displayed in Table 1.

The association constants with the single porphyrin species are all in the same range and, as expected, rather weak. Among the bis-porphyrin

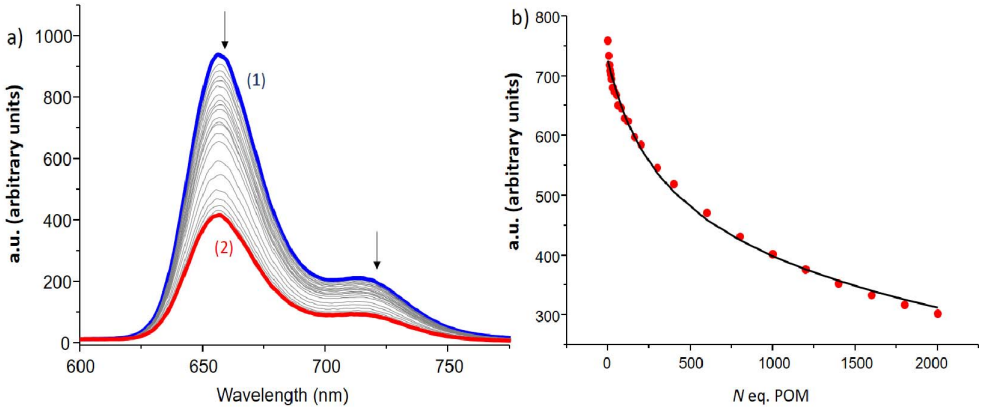

Figure 6. (a) Fluorescence titration of **6** with $[Mo_6O_{19}][(n\text{-Bu})_4N]_2$. Solvent: DMF, T = 25.0 °C, λ_{ex} = 517 nm, emission and excitation slits 15/20 nm, (1) [**6**] = 4.39×10^{-6} M; (2) [POM] / [**6**] = 2000. (b) Monitoring of the emission intensity at 657 nm as a function of the number of equivalents $[Mo_6O_{19}][(n\text{-Bu})_4N]_2$. The emission spectra are not corrected from dilution effects.

receptors, **9** emerges being by far the best receptor for a Lindqvist-type guest. Although the Spartan™ model suggest an ideal porphyrin–porphyrin distance in the 11 to 14 Å range that is too large for the terminal oxygen atoms spacing in a Lindqvist-type polyoxometalate, the difference in stability may be explained by a stronger interaction of the oxygen atoms with the *m*-pyridinium charges in **9**. A better wrapping of the porphyrins around the POM would release two PF_6^- anions and the corresponding entropy gain could account for the 2 orders of magnitude enhancement of the association. In comparison, for a similar positioning of the pyridinium charges in **10**, the longer spacer must still allow a stronger and thus more organized interaction of the counter anions with the host–guest complex. As a result of the binding studies described above, the **9**:POM species has been selected to investigate the properties of the porphyrin/POM scaffolds.

4. Electrochemisty and photophysical properties of 9:POM species

The binary complex **9**-POM has been selected to determine the nature of both the interactions and the quenching observed in solution. As shown by the series of voltammograms in Figure 7, the trace of the bis-porphyrin reduction is unaffected by the addition of POM in the millimolar concentration range. This observation suggests the absence of electronic interactions between the host and the guest in the ground state, confirming the absence of spectral changes that hampered an easy determination of the association constants by UV–Vis means. The values of the redox couples observed in Figure 7 allow prediction of the energy levels involved in a photo-induced electron transfer in any porphyrin/POM donor/acceptor scaffold.

The two modes of quenching, static and dynamic, are represented in Figure 8, together with the associated energy diagram of the oxidative quenching of the porphyrin excited state. In a static quenching process, the fluorescence decrease is caused by the lesser number of fluorescent chromophores when the quencher is present that transduces in a lower fluorescence quantum yield but the kinetic constants associated to the relaxation of the excited state remain unchanged. As a result, the excited state lifetime does not vary upon changes in the concentration of the quencher, which is typical of the formation of a non-fluorescent host–guest complex [19]. When the quenching results from a dynamic process, the rising of a new deactivation pathway affects the relaxation of the excited state and both the fluorescence quantum yield and the lifetime of the excited state vary upon the quencher concentration changes [20].

As shown in the Figure 9, neither the profile nor the time scale of the decay show any alteration upon the addition of POM to the fluorescent dimer **9**.

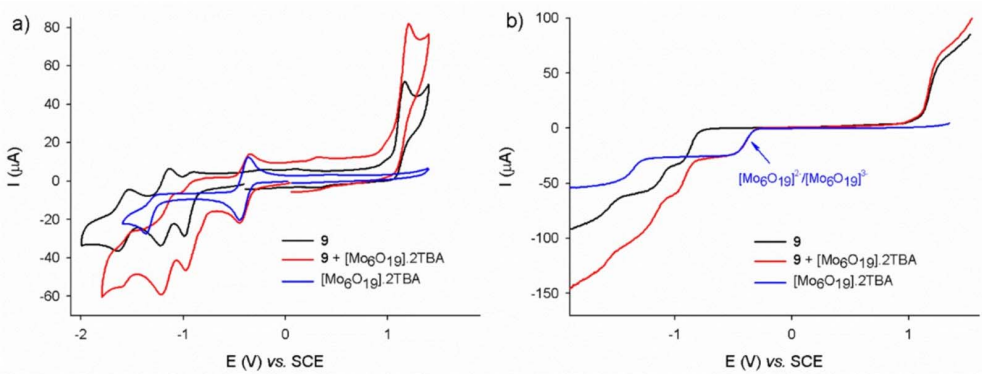

Figure 7. (a) Cyclic voltammogram of the porphyrin dimer **9** (black trace), of $[[Mo_6O_{19}][(n\text{-}Bu)_4N]_2$ (blue trace) and a mixture of **9** + $[Mo_6O_{19}][(n\text{-}Bu)_4N]_2$ (red trace), conditions: DMF 0.1 M NBu_4PF_6, [**9**] = $[Mo_6O_{19}][(n\text{-}Bu)_4N]_2$ = 0.80 mM. Scan rate: v = 100 mV·s^{-1}. (b) Corresponding stationary voltamperometry: v = 10 mV·s^{-1}, working electrode: glassy carbon (d = 3 mm), internal reference: Fc (not shown).

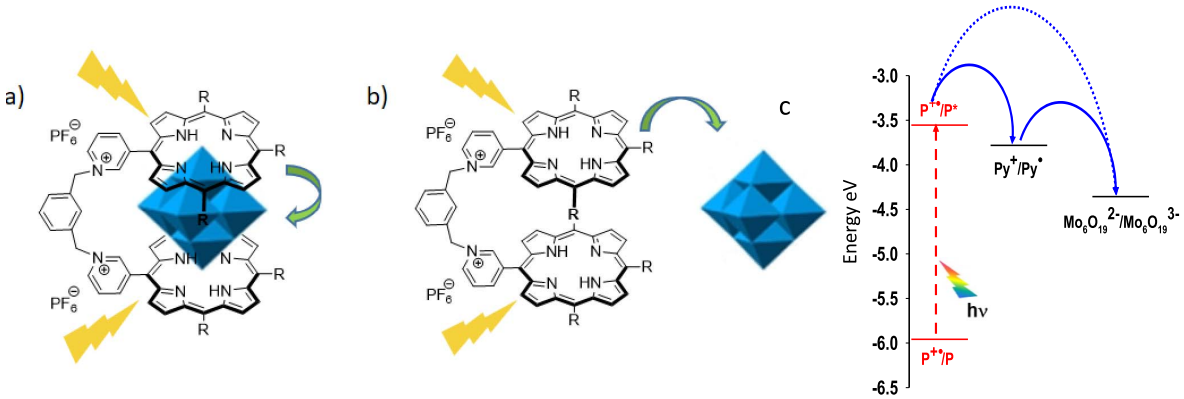

Figure 8. Idealized representation of the oxidative (a) static fluorescence quenching and (b) dynamic fluorescence quenching of porphyrins in the dimer **9** by a Lindqvist-type polyoxometalate; (c) energy diagram of the subsequent electron transfer. P = porphyrin.

Table 2. Lifetime values for dimer **9** as a function of $[Mo_6O_{19}][(Bu_4N)_2]$ equivalents (10% error margin)

POM equivalents	0	2.5	5	18	36	72	184	368
Lifetime (ns)	10.1	9.94	9.77	9.51	9.27	9.53	9.86	9.80

Table 2 summarizes the small changes (average: 6%) observed for the lifetime of **9** which are assigned to small dilution effects and largely within the standard errors (10%).

These results clearly show that the partial fluorescence extinction is caused by the formation of a host–guest complex between **9** and the POM in their ground state and not by a dynamic process or an electron transfer in the excited state.

5. Conclusion

In this work, several dicationic bis-porphyrins have been prepared as receptors for polyoxometalate anions. The receptors show various positioning and spacing of their positive charge and, to the one exception of **9**, only moderate affinities for a Lindqvist-type polyoxometalate. As a result, it is fair to assume that electrostatic interactions taken for granted

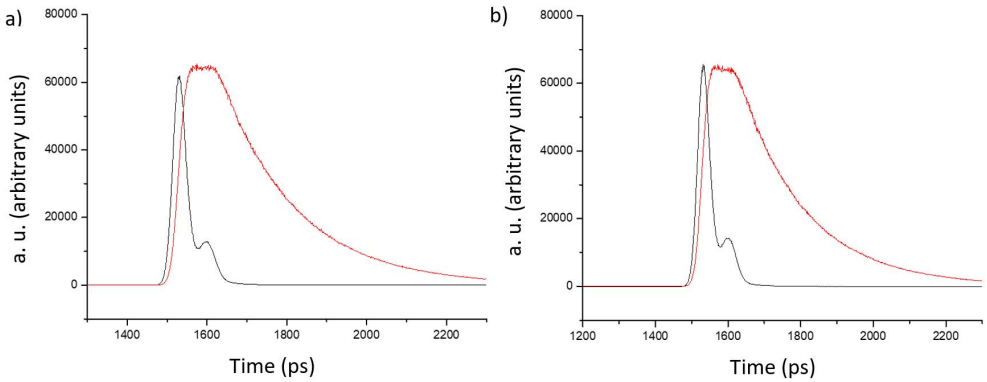

Figure 9. Excitation pulse (black trace) and decay of the fluorescing species (red trace): (a) dimer **9**, (b) dimer **9** and 368 equivalents of $[Mo_6O_{19}][(n\text{-Bu})_4N]_2$. Solvent DMF, T = 25.0 °C, λ_{ex} = 517 nm, [**9**] = 6.43×10^{-6} M.

in most self-assembling methods for the formation of porphyrin-POM scaffolds are subject to geometric requirements. Thus without the knowledge of the precise structure of the porphyrin-POM assembly, the rationalization of the behaviour and the structure/properties relationships remains difficult, if not unreliable. In the case of the most stable host–guest complex **9-POM**, it has been shown that a quenching of the excited state of the bis-porphyrin is due to the formation of a host–guest complex because the lifetime of the fluorescent species itself remains unaffected. To rationalize all parameters, receptors with different spacers and the use of charged metalloporphyrins instead of free bases needs to be performed. At the moment, the investigation of the affinities of all other porphyrin dimers described in this work for variously shaped POMs such as Keggin and Anderson is in progress in order to extract parameters relevant to the host–guest interactions.

6. Experimental section

6.1. *General methods*

Dichloromethane used for reactions or column chromatography was distilled from calcium hydride. Tetrahydrofuran and toluene were distilled over sodium/benzophenone ketyl under argon. All other commercially available reagents and solvents were used without further purification. Bases (K_3PO_4, K_2CO_3, Cs_2CO_3 and Na_2CO_3) were oven-dried at 100 °C. Analytical thin layer chromatography (TLC) was carried out on silica gel 60 F_{254} (Merck) and column chromatography was performed with silica gel or alumina from Merck (alumina oxide 60 standardized or silica gel 60, 0.04–0.063 µm). Nuclear magnetic resonance spectra were recorded on Bruker Avance spectrometers at 300, 400, 500 or 600 MHz. The chemical shifts are given in parts-per-million (ppm) on the delta scale. The solvent peak was used as reference value: for ^{1}H NMR: $CDCl_3$ = 7.26 ppm, DMSO-d_6 = 2.50 ppm, for ^{13}C NMR: $CDCl_3$ = 77.23 ppm, DMSO-d_6 = 39.52 ppm. The data are presented as follows: chemical shift, multiplicity (s = singlet, d = doublet, t = triplet, q = quartet, hept = heptuplet, m = multiplet), coupling constant (J/Hz) and the integration. Mass spectra were obtained by ESI-TOF or MALDI-TOF (337 nm nitrogen laser for desorption, dithranol used as matrix) experiments. High resolution mass spectra (HRMS) data were recorded on a microTOF spectrometer equipped with orthogonal electrospray interface (ESI). The ions (*m/z*) were analyzed on a Bruker Daltonics microTOF for ESI and a Bruker Autoflex II TOF-TOF for MALDI. The parent ions, $[M+H]^+$, $[M+K]^+$, $[M+Na]^+$ or $[M^{n+}]$ are given. UV–visible spectra were recorded on a Cary 5000 UV/vis/NIR double-beam spectrometer in dichloromethane, chloroform or DMF. Molar extinction coefficients were determined for samples with analyte concentrations ranging from 5×10^{-6} to 5×10^{-5} mol·L^{-1}.

Binding studies were carried out with spectroscopic grade DMF (Carlo Erba, 99.9% for spectroscopy). To prevent any photochemical degradation, all solutions were protected from daylight expo-

sure. All stock solutions were prepared using a Mettler Toledo XA105 Dual Range (0.01/0.1 mg–41/120 g) to weigh samples, and complete dissolution in DMF was achieved using an ultrasonic bath. The concentrations of stock solutions of the receptors and substrates were calculated by the quantitative dissolution of solid samples in DMF.

Luminescence titrations were carried out on solutions of dimers and monomers with absorbances lower than 0.1. The titrations of 2 mL of dimer or monomer with $[Mo_6O_{19}][(Bu_4N)_2]$ ([Dimers] = 6.43×10^{-6} M and [Monomers] = 4.39×10^{-6} M) were carried out in a 1 cm Hellma quartz optical cell by the addition of known microvolumes of solutions of $[Mo_6O_{19}][(Bu_4N)_2]$ with an Eppendorf Research plus. The excitation wavelengths were set at 517 or 559 nm. The luminescence spectra were recorded from 550 to 800 nm on a PerkinElmer LS-50B instrument maintained at 25 °C. The slit widths were set between 15 and 20 nm for the emission. Luminescence titrations were conducted under precise and identical experimental conditions.

The spectrophotometric titration of **9** with $[Mo_6O_{19}][(Bu_4N)_2]$ ([**9**] = 1.76×10^{-2} M) was carried out in a 1 cm Hellma quartz optical cell by the addition of known microvolumes of solutions of $[Mo_6O_{19}][(Bu_4N)_2]$ with an Eppendorf Research plus. Special care was taken to ensure that complete equilibration was attained. The corresponding UV–Vis spectra were recorded from 300 to 800 nm on a Cary 5000 (Agilent) spectrophotometer maintained at 25 °C.

The spectrophotometric data were analyzed with Specfit [21] program that adjusts the absorptivities and the stability constants of the species formed at equilibrium. Specfit uses factor analysis to reduce the absorbance matrix and to extract the eigenvalues prior to the multi-wavelength fit of the reduced data set according to the Marquardt algorithm [22,23].

6.2. *General procedure for the single porphyrin derivatives **3**–**6** (GP1)*

A mixture of porphyrin **1** or **2** and the α,α'-dibromo-xylene corresponding in THF (15 mL) was refluxed for 6 h under argon atmosphere. Water was added to the reaction mixture. The organic layer was separated, and the aqueous layer was extracted with CH_2Cl_2 (20 mL). The organic layer was washed with water, dried over Na_2SO_4 and the solvent removed under vacuum. The crude product was recrystallized three times (addition of saturated KPF_6 aqueous solution to acetone solution). The precipitate was filtered, washed with water and solubilized in acetone. The acetone was then removed under vacuum.

6.2.1. *Porphyrin **3***

Prepared following the **GP1** and using α,α'-dibromo-m-xylene(160 mg, 1.60 mmol, 20 eq) and porphyrin **1** (50 mg, 0.08 mmol, 1 eq). The crude product was purified by silica gel column chromatography (CH_2Cl_2) and gradually ending with CH_2Cl_2/Acetone (9/1). The compound **3** (73 mg, 0.071 mmol, 87%) was obtained as a purple solid. ^{1}H NMR (500 MHz, Acetone-d_6): δ 9.73 (d, J = 6.6 Hz, 2H, H-*ortho*-py$^+$), 9.16 (d, J = 6.6 Hz, 2H, H-*meta*-py$^+$), 9.03–8.84 (m, 8H, H-β-pyrrolic), 8.23–8.06 (m, 6H, H-tolyl), 7.93 (s, 1H), 7.81 (dt, J = 7.0, 2.0 Hz, 1H), 7.68 (d, J = 7.7 Hz, 6H, H-tolyl), 7.65–7.59 (m, 2H), 6.43 (s, 2H, Py$^+$–**CH**$_2$–Ar), 4.81 (d, J = 5.5 Hz, 2H, Ar–**CH**$_2$–Br), 2.72 (s, 9H, –CH$_3$), −2.72 (s, 2H, free base). ^{13}C NMR (11 MHz, Acetone-d_6) δ 161.1, 145.4, 144.3, 139.2, 139.1, 139.0, 135.4, 134.8, 134.4, 130.6, 129.2, 129.1, 128.7, 128.7, 128.7, 123.7, 123.7, 122.5, 122.5, 113.1, 64.3, 27.6, 21.7. ^{31}P NMR (203 MHz, Acetone-d_6) δ −144.0 (hept, J = 711.7 Hz). ^{19}F NMR (471 MHz, Acetone-d_6) δ −72.6 (d, J = 711.7 Hz). UV–Vis (DMF): λ (ε) = 419 (223000), 516 (12700), 552 (7700), 591 (5700), 647 nm (4100 $M^{-1}\cdot cm^{-1}$). ESI-TOF: m/z = 840.27 Calcd for $C_{54}H_{43}N_5Br$ ([M$^+$]): 840.27. TLC (silica) R_f: 0.25 (CH_2Cl_2/Acetone 9/1).

6.2.2. *Porphyrin **4***

Prepared following the **GP1** and using α,α'-dibromo-m-xylene (160 mg, 1.60 mmol, 20 eq) and porphyrin **1** (50 mg, 0.08 mmol, 1 eq). The crude product was purified by silica gel column chromatography (CH_2Cl_2 and gradually ending with CH_2Cl_2/Acetone 9/1). The compound **4** (76 mg, 0.073 mmol, 91%) was obtained as a purple solid. ^{1}H NMR (400 MHz, Acetone-d_6): δ 9.72 (d, J = 6.8 Hz, 2H, H-*ortho*-py$^+$), 9.16 (d, J = 6.8 Hz, 2H, H-*meta*-py$^+$), 9.03–8.95 (m, 4H, H-β-pyrrolic), 8.91 (q, J = 4.9 Hz, 4H, H-β-pyrrolic), 8.17–8.06 (m, 6H, H-tolyl), 7.94 (d, J = 8.0 Hz, 2H), 7.75 (d, J = 8.0 Hz, 2H), 7.69–7.59 (m, 6H, H-tolyl), 6.43 (s, 2H, Py$^+$–CH$_2$–Ar), 4.78 (s, 2H, Ar–CH$_2$–Br), 2.70 (s, 6H, –CH$_3$), 2.69 (s, 3H, –CH$_3$), −2.73 (s, 2H, free base). ^{13}C NMR (126 MHz,

Acetone-d_6): δ −72.5 (d, J = 707.7 Hz). ^{31}P NMR (121 MHz, Acetone-d_6): δ −144.2 (hept, J = 707.7 Hz). ^{19}F NMR (282 MHz, Acetone-d_6): δ 160.9, 144.2, 141.2, 139.5, 138.8, 135.2, 134.5, 134.5, 131.3, 131.0, 128.5, 128.5, 123.4, 122.3, 113.0, 65.0, 33.4, 27.5, 21.5. UV–Vis (DMF): λ (ε) = 421 (314000), 518 (19000), 556 (11800), 592 (7300), 649 nm (6600 $M^{-1}\cdot cm^{-1}$). HRMS, ESI-TOF: m/z = 840.2685 Calcd for $C_{54}H_{43}BrN_5^+$ ([M$^+$]): 840.2696. TLC R_f: 0.24 (CH_2Cl_2/Acetone 9/1).

6.2.3. *Porphyrin **5***

Prepared following the **GP1** and using α,α'-dibromo-m-xylene (160 mg, 1.60 mmol, 20 eq) and porphyrin **2** (50 mg, 0.08 mmol, 1 eq). The crude product was purified by silica gel column chromatography (CH_2Cl_2) and gradually ending with CH_2Cl_2/Acetone (9/1). The compound **5** (68 mg, 0.065 mmol, 79%) was obtained as a purple solid. ^{1}H NMR (400 MHz, Acetone-d_6): δ 10.21 (m, 1H, H-py$^+$), 9.79 (dt, J = 6.2, 1.5 Hz, 1H, H-py$^+$), 9.60 (dt, J = 8.0, 1.5 Hz, 1H, H-py$^+$), 9.04–8.88 (m, 8H, H-β-pyrrolic), 8.81 (dd, J = 8.1, 6.2 Hz, 1H, H-py$^+$), 8.18–8.07 (m, 2H, H-tolyl), 7.97 (br s, 1H) 7.83 (dd, J = 7.6, 1.6 Hz, 1H), 7.70–7.61 (m, 7H, H-tolyl), 7.58–7.55 (m, 1H, H3), 6.45 (s, 2H, Py$^+$–CH_2–Ar), 4.68 (s, 2H, Ar–CH_2–Br), 2.71 (s, 3H, –CH_3), 2.70 (s, 6H, –CH_3), −2.78 (s, 2H, free base). ^{13}C NMR (126 MHz, Acetone-d_6): δ 150.1, 148.1, 145.2, 144.0, 140.8, 139.5, 139.5, 138.8, 135.2, 131.5, 130.9, 130.9, 130.2, 128.5, 128.5, 128.3, 123.1, 122.1, 110.6, 65.7, 33.5, 21.5. ^{31}P NMR (121 MHz, Acetone-d_6): δ −144.3 (hept, J = 707.5 Hz). ^{19}F NMR (282 MHz, Acetone-d_6): δ −72.60 (d, J = 707.5 Hz). UV–Vis (DMF): λ (ε) = 422 (312000), 517 (18000), 552 (8900), 591 (6400), 649 nm (5700 $M^{-1}\cdot cm^{-1}$). HRMS, ESI-TOF: m/z = 840.2658 Calcd for $C_{54}H_{43}BrN_5^+$ ([M$^+$]): 840.2696. TLC R_f: 0.19 (CH_2Cl_2/Acetone 9/1).

6.2.4. *Porphyrin **6***

Prepared following the **GP1** and using α,α'-dibromo-p-xylene (160 mg, 1.60 mmol, 20 eq) and porphyrin **2** (50 mg, 0.08 mmol, 1 eq). The crude product was purified by silica gel column chromatography (CH_2Cl_2) and gradually ending with CH_2Cl_2/Acetone(9/1). The compound **6** (72 mg, 0.07 mmol, 86%) was obtained as a purple solid. ^{1}H NMR (400 MHz, Acetone-d_6): δ 10.19 (s, 1H, H-py$^+$), 9.79 (d, J = 6.2 Hz, 1H, H-py$^+$), 9.59 (d, J = 7.9 Hz, 1H, H-py$^+$), 9.10–8.87 (m, 8H, H-β-pyrrolic), 8.80 (dd, J = 7.9, 6.2 Hz, 1H, H-py$^+$), 8.21–8.06 (m, 6H, H-tolyl), 7.86 (d, J = 8.1 Hz, 2H), 7.74–7.58 (m, 8H, H-tolyl), 6.44 (s, 2H, Py$^+$–CH_2–Ar), 4.69 (s, 2H, Ar–CH_2–Br), 2.71 (s, 6H, –CH_3), 2.71 (s, 3H, –CH_3), −2.78 (s, 2H, free base). ^{13}C NMR (126 MHz, Acetone-d_6): δ 50.1, 148.2, 145.2, 139.5, 138.8, 135.2, 134.7, 131.2, 130.8, 128.5, 128.5, 128.3, 123.1, 122.1, 65.6, 33.3, 21.5. ^{31}P NMR (121 MHz, Acetone-d_6): δ −141.3 (hept, J = 707.5 Hz). ^{19}F NMR (282 MHz, Acetone-d_6): δ −72.6 (d, J = 707.5 Hz). UV–Vis (DMF): λ (ε) = 422 (314000), 517 (17500), 552 (8500), 591 (6000), 649 nm (5200 $M^{-1}\cdot cm^{-1}$). HRMS, ESI-TOF: m/z = 840.2644 Calcd for $C_{54}H_{43}BrN_5^+$ ([M$^+$]): 840.2696. TLC R_f: 0.23 (CH_2Cl_2/Acetone 9/1).

6.3. *General procedure for the bis-porphyrin **7**–**10** (GP2)*

6.3.1. *Method A*

A mixture of monomeric porphyrin and porphyrins **1** or **2** in THF (5 mL) was refluxed for 30 h under argon atmosphere. Water was added to the reaction mixture. The organic layer was separated, and the aqueous layer was extracted with CH_2Cl_2 (20 mL). The organic layer was washed with water, dried over Na_2SO_4 and the solvent removed under vacuum. The crude product was recrystallized three times (addition of saturated KPF_6 aqueous solution to acetone solution). The precipitate was filtered, washed with water and solubilized in acetone. The acetone was removed under vacuum.

6.3.2. *Method B*

A mixture of porphyrin **1** or **2** and the α,α'-dibromo-xylene corresponding in THF (15 mL) was refluxed for 38 h under argon atmosphere. Water was added to the reaction mixture. The organic layer was separated, and the aqueous layer was extracted with CH_2Cl_2 (20 mL). The organic layer was washed with water, dried over Na_2SO_4 and the solvent removed under vacuum. The crude product was recrystallized three times (addition of saturated KPF_6 aqueous solution to acetone solution). The precipitate was filtered, washed with water and solubilized in acetone. The acetone was removed under vacuum.

6.3.3. *Bis-porphyrin **7***

Prepared following the **GP2** and using monomeric systems (61 mg, 0.062 mmol, 1 eq) (Method A) or

α,α'-Dibromo-m-xylene (18 mg, 0.062 mmol, 1 eq) (Method B) and porphyrin **1** (204 mg, 0.31 mmol, 5 eq). The crude product was purified by silica gel column chromatography (CH_2Cl_2) and gradually ending with a solution of KPF_6 (27 mM) in acetone. The compound **7** (80 mg, 0.047 mmol, 75%, Method A) or (49 mg, 0.029 mmol, 46%, Method B) was obtained as a purple solid. ^{1}H NMR (500 MHz, DMSO-d_6,): δ 9.62 (d, J = 6.0 Hz, 4H, H-*ortho*-py$^+$), 9.12 (d, J = 6.0 Hz, 4H, H-*meta*-py$^+$), 8.83 (d, J = 4.5 Hz, 4H, H-β-pyrrolic), 8.74 (d, J = 4.5 Hz, 4H, H-β-pyrrolic), 8.38 (d, J = 4.7 Hz, 4H, H-β-pyrrolic), 8.35 (d, J = 4.7 Hz, 4H, H-β-pyrrolic), 8.24 (s, 1H), 8.12–8.02 (m, 6H, H-*ortho*-tolyl), 7.89 (d, J = 7.7 Hz, 1H), 7.65 (d, J = 7.4 Hz, 4H, H-*meta*-tolyl), 7.01 (d, J = 7.3 Hz, 8H, H-*ortho*-tolyl), 6.69 (d, J = 7.3 Hz, 8H, H-*meta*-tolyl), 6.33 (s, 4H, –CH_2–), 2.69 (s, 6H, –CH_3), 2.24 (s, 12H, –CH_3), −3.06 (s, 4H, free base). ^{13}C NMR (126 MHz, DMSO-d_6): δ 158.5, 143.4, 138.1, 137.6, 137.3, 136.7, 135.5, 134.2, 133.4, 132.8, 131.0, 130.4, 129.7, 127.7, 126.9, 121.7, 120.3, 112.4, 63.1, 21.1, 20.6. ^{31}P NMR (121 MHz, DMSO-d_6): δ −144.2 (hept, J = 711.3 Hz). ^{19}F NMR (282 MHz, DMSO-d_6): δ −70.1 (d, J = 711.3 Hz). UV–Vis (DMF): λ (ε) = 419 (198000), 516 (11300), 552 (6300), 591 (4500), 648 nm (3700 $M^{-1}\cdot cm^{-1}$). ESI-TOF: m/z = 709.83 Calcd for $C_{100}H_{78}N_{10}^{2+}$ ([M^{2+}]): 709.32. TLC R_f: 0.26 (solution of KPF_6 (27 mM) in Acetone).

6.3.4. *Bis-porphyrin **8***

Prepared following the **GP2** and using monomeric systems (61 mg, 0.062 mmol, 1 eq) (Method A) or α,α'-Dibromo-p-xylene (18 mg, 0.062 mmol, 1 eq) (Method B) and porphyrin **1** (204 mg, 0.31 mmol, 5 eq). The crude product was purified by silica gel column chromatography (CH_2Cl_2) and gradually ending with a solution of KPF_6 (27 mM in acetone). The compound **8** (72 mg, 0.042 mmol, 68%, Method A) or (40 mg, 0.024 mmol, 38%, Method B) was obtained as a purple solid. ^{1}H NMR (400 MHz, DMSO-d_6): δ 9.66 (d, J = 6.2 Hz, 4H, H-*ortho*-py$^+$), 9.12 (d, J = 6.2 Hz, 4H, H-*meta*-py$^+$), 9.06–8.99 (m, 4H, H-β-pyrrolic), 8.97–8.92 (m, 4H, H-β-pyrrolic), 8.90–8.81 (m, 8H, H-β-pyrrolic), 8.11 (s, 4H, H-aryl), 8.10–8.04 (m, 12H, H-*ortho*-tolyl), 7.65 (d, J = 7.8 Hz, 8H, H-*meta*-tolyl), 7.61 (d, J = 7.8 Hz, 4H, H-*meta*-tolyl), 6.28 (s, 4H, –CH_2–), 2.68 (s, 6H, –CH_3), 2.64 (s, 12H, –CH_3), −2.89 (s, 4H, free base). ^{13}C NMR (126 MHz, DMSO-d_6): δ 158.8, 143.8, 138.5, 138.2, 138.2, 138.1, 138.0, 136.5, 135.9, 134.6, 133.7, 130.8, 128.2, 122.5, 121.4, 113.1, 111.1, 69.0, 30.1, 21.6, 21.5. ^{31}P NMR (121 MHz, DMSO-d_6): δ −141.27 (hept, J = 711.3 Hz). ^{19}F NMR (282 MHz, DMSO-d_6): δ −70.14 (d, J = 711.3 Hz). UV–Vis (DMF): λ (ε) = 422 (354000), 518 (37600), 556 (29200), 592 (22400), 650 nm (19300 $M^{-1}\cdot cm^{-1}$). HR-ESI-TOF: m/z = 709.8236 Calcd for $C_{100}H_{78}N_{10}^{2+}$ ([M^{2+}]): 709.8216. TLC R_f: 0.31 (solution of KPF_6 (5 mM) in Acetone).

6.3.5. *Bis-porphyrin **9***

Prepared following the **GP2** and using monomeric systems (61 mg, 0.062 mmol, 1 eq) (Method A) or α,α'-Dibromo-m-xylene (18 mg, 0.062 mmol, 1 eq) (Method B) and porphyrin **2** (204 mg, 0.31 mmol, 5 eq). The crude product was purified by silica gel column chromatography (CH_2Cl_2) and gradually ending with a solution of KPF_6 (27 mM in acetone). The compound **9** (67 mg, 0.039 mmol, 63%, Method A) or (51 mg, 0.030 mmol, 48%, Method B) was obtained as a purple solid. ^{1}H NMR (400 MHz, DMSO-d_6): δ 10.19 (s, 2H, H-py$^+$), 9.62 (d, J = 6.5 Hz, 2H, H-py$^+$), 9.38 (d, J = 7.9 Hz, 2H, 2H, H-py$^+$), 8.89–8.79 (m, 8H, H-β-pyrrolic), 8.75–8.65 (m, 8H, H-β-pyrrolic), 8.54 (dd, J = 7.9, 6.5 Hz, 2H, H-py$^+$), 8.13–8.05 (m, 4H, H-tolyl), 8.01 (s, 1H), 7.86 (d, J = 7.7 Hz, 2H), 7.80 (d, J = 7.3 Hz, 4H, H-tolyl), 7.71 (t, J = 7.7 Hz, 1H), 7.69–7.59 (m, 8H, H-tolyl), 7.40 (d, J = 7.3 Hz, 4H, H-tolyl), 7.22 (d, J = 7.8 Hz, 4H, H-tolyl), 6.21 (s, 4H, –CH_2–), 2.68 (s, 6H, –CH_3), 2.49 (s, 12H, –CH_3), −3.01 (s, 4H, free base). ^{13}C NMR (126 MHz, DMSO-d_6): δ 1148.9, 147.0, 144.4, 141.6, 138.1, 137.8, 137.7, 137.6, 137.4, 135.4, 134.2, 134.0, 133.9, 133.8, 130.5, 130.2, 130.2, 130.2, 129.3, 127.8, 127.7, 127.6, 127.6, 127.4, 127.0, 121.7, 120.6, 110.2, 104.9, 55.9, 32.2, 29.6, 21.1, 20.9. ^{31}P NMR (121 MHz, DMSO-d_6): δ −144.2 (hept, J = 711.3 Hz). ^{19}F NMR (282 MHz, DMSO-d_6): δ −70.1 (d, J = 711.3 Hz). UV–Vis (DMF): λ (ε) = 422 (154000), 516 (9800), 552 (4700), 590 (3600), 647 nm (2500 $M^{-1}\cdot cm^{-1}$). HR-ESI-TOF: m/z = 709.8220 Calcd for $C_{100}H_{78}N_{10}^{2+}$ ([M^{2+}]): 709.8216. TLC R_f: 0.21 (solution of KPF_6 (5 mM) in Acetone).

6.3.6. *Bis-porphyrin **10***

Prepared following the **GP10** and using monomeric systems (61 mg, 0.062 mmol, 1 eq) (Method A) or α,α'-Dibromo-p-xylene (18 mg, 0.062 mmol, 1 eq) (Method B) and porphyrin **2** (204 mg,

0.31 mmol, 5 eq). The crude product was purified by silica gel column chromatography (CH_2Cl_2) and gradually ending with a solution of KPF_6 (27 mM in acetone). The compound **10** (76 mg, 0.044 mmol, 71%, Method A) or (34 mg, 0.020 mmol, 32%, Method B) was obtained as a purple solid. ^{1}H NMR (500 MHz, DMSO-d_6): δ 10.26 (s, 2H, H-py$^+$), 9.71 (d, J = 6.3 Hz, 2H, H-py$^+$), 9.39 (d, J = 7.9 Hz, 2H, H-py$^+$), 8.88–8.82 (m, 8H, H-β-pyrrolic), 8.77–8.69 (m, 8H, H-β-pyrrolic), 8.64 (dd, J = 7.9, 6.3 Hz, 2H, H-py$^+$), 8.15–8.04 (m, 4H, H-tolyl), 7.91 (s, 4H, H-aryl), 7.83 (d, J = 7.7 Hz, 4H, H-tolyl), 7.70–7.58 (m, 8H, H-tolyl), 7.34 (d, J = 7.7 Hz, 4H, H-tolyl), 7.15 (d, J = 7.7 Hz, 4H, H-tolyl), 6.17 (s, 4H, –CH_2–), 2.68 (s, 6H, –CH_3), 2.41 (s, 12H, –CH_3), −2.97 (s, 4H, free base). ^{13}C NMR (126 MHz, DMSO-d_6): δ 162.3, 148.7, 147.0, 144.4, 141.6, 138.1, 137.8, 137.6, 137.3, 135.7, 134.2, 134.0, 133.8, 133.8, 129.8, 127.7, 127.5, 127.4, 127.2, 121.7, 120.7, 110.3, 63.3, 55.8, 35.8, 30.8, 21.1, 20.8. ^{31}P NMR (121 MHz, DMSO-d_6): δ −144.2 (hept, J = 711.3 Hz). ^{19}F NMR (282 MHz, DMSO-d_6): δ −70.1 (d, J = 711.3 Hz). UV–Vis (DMF): λ (ε) = 420 (101000), 516 (8500), 552 (5900), 590 (4800), 649 nm (4200 $M^{-1}\cdot cm^{-1}$). HR-ESI-TOF: m/z = 709.3229 Calcd for $C_{100}H_{78}N_{10}^{2+}$ ([M^{2+}]): 709.3200. TLC R_f: 0.28 (solution of KPF_6 (5 mM) in acetone).

Acknowledgments

The authors are grateful to the University of Strasbourg and the CNRS for constant financial support. RL gratefully acknowledges the Région Grand-Est and the Fondation Recherche en Chimie for a PhD fellowship. The authors declare no conflicts of interest.

Supplementary data

Supporting information for this article is available on the journal's website under https://doi.org/10.5802/crchim.105 or from the author.

References

[1] I. Azcarate, Z. Huo, R. Farha, M. Goldmann, H. Xu, B. Hasenknopf, E. Lacôte, L. Ruhlmann, *Chem. Eur. J.*, 2015, **21**, 8271-8280.

[2] J. Hao, A. Giraudeau, Z. Ping, L. Ruhlmann, *Langmuir*, 2008, **24**, 1600-1603.

[3] Q. Chen, D. P. Goshorn, C. P. Scholes, X. L. Tan, J. Zubieta, *J. Am. Chem. Soc.*, 1992, **114**, 4667-4681.

[4] W. H. Knoth, R. L. Harlow, *J. Am. Chem. Soc.*, 1981, **103**, 4265-4266.

[5] K. J. Elliott, A. Harriman, L. Le Pleux, Y. Pellegrin, E. Blart, C. R. Mayer, F. Odobel, *Phys. Chem. Chem. Phys.*, 2009, **11**, 8767-8773.

[6] F. Odobel, M. Séverac, Y. Pellegrin, E. Blart, C. Fosse, C. Cannizzo, C. R. Mayer, K. J. Elliott, A. Harriman, *Chem.–Eur. J.*, 2009, **15**, 3130-3138.

[7] Y. Zhu, Y. Huang, Q. Li, D. Zang, J. Gu, Y. Tang, Y. Wei, *Inorg. Chem.*, 2020, **59**, 2575-2583.

[8] D. Schaming, C. Costa-Coquelard, I. Lampre, S. Sorgues, M. Erard, X. Liu, J. Liu, L. Sun, J. Canny, R. Thouvenot, L. Ruhlmann, *Inorg. Chim. Acta*, 2010, **363**, 2185-2192.

[9] A. Yokoyama, K. Ohkubo, T. Ishizuka, T. Kojima, S. Fukuzumi, *Dalton Trans.*, 2012, **41**, 10006-10013.

[10] C. Li, N. Mizuno, K. Yamaguchi, K. Suzuki, *J. Am. Chem. Soc.*, 2019, **141**, 7687-7692.

[11] C. Costa-Coquelard, S. Sorgues, L. Ruhlmann, *J. Phys. Chem. A*, 2010, **114**, 6394-6400.

[12] S.-Q. Liu, J.-Q. Xu, H.-R. Sun, D.-M. Li, *Inorg. Chim. Acta*, 2000, **306**, 87-93.

[13] I. Ahmed, R. Farha, M. Goldmann, L. Ruhlmann, *Chem. Commun.*, 2013, **49**, 496-498.

[14] C. Li, K.-M. Park, H.-J. Kim, *Inorg. Chem. Commun.*, 2015, **60**, 8-11.

[15] Z. Shi, Y. Zhou, L. Zhang, C. Mu, H. Ren, D. ul Hassan, D. Yang, H. M. Asif, *RSC Adv.*, 2014, **4**, 50277-50284.

[16] G. Bazzan, W. Smith, L. C. Francesconi, C. M. Drain, *Langmuir*, 2008, **24**, 3244-3249.

[17] R. Lamare, L. Ruhlmann, R. Ruppert, J. Weiss, *J. Porphyr. Phthalocyanines*, 2019, **23**, 860-868.

[18] A. L. Rheingold, C. B. White, B. S. Haggerty, E. A. Maatta, *Acta Crystallogr. C*, 1993, **49**, 756-758.

[19] A. C. Vaiana, H. Neuweiler, A. Schulz, J. Wolfrum, M. Sauer, J. C. Smith, *J. Am. Chem. Soc.*, 2003, **125**, 14564-14572.

[20] L. K. Fraiji, D. M. Hayes, T. C. Werner, *J. Chem. Educ.*, 1992, **69**, 424-428.

[21] H. Gampp, M. Maeder, C. J. Meyer, A. D. Zuberbühler, *Talanta*, 1985, **32**, 95-101.

[22] D. W. Marquardt, *J. Soc. Ind. Appl. Math.*, 1963, **11**, 431-441.

[23] M. Maeder, A. D. Zuberbuehler, *Anal. Chem.*, 1990, **62**, 2220-2224.